DMD #1842

Metabolic Activation of Fluoropyrrolidine Dipeptidyl Peptidase-IV Inhibitors by Rat Liver Microsomes

Shiyao Xu, Bing Zhu, Yohannes Teffera, Deborah E. Pan, Charles G. Caldwell, George Doss, Ralph A. Stearns, David C. Evans, and Maria G. Beconi

Department of Drug Metabolism (S.X., B.Z., Y.T., D.E.P., G.D., R.A.S., D.C.E., M.G.B.), and Medicinal Chemistry (C.G.C), Merck Research Laboratories, P.O.Box 2000, Rahway, NJ 07065

Y.T. current address: DMPK, Amgen – Cambridge Research Center, Cambridge, MA 02139

M.G. B. current address: RI-CEDD, Glaxo Smith Kline, King of Prussia, PA 19406

Running Title: Metabolic bioactivation of fluoropyrrolidine derivatives

Address correspondence to:
Shiyao Xu, Ph.D.
Department of Drug Metabolism
Merck Research Laboratories
P.O.Box 2000, RY80E-200
Rahway, NJ 07065-0900
Phone #: (732)594-7635
Fax #: (732)594-1416
E-mail: shiyao_xu@merck.com

Text pages: 22
Tables: 2
Figures: 8
Schemes: 1
References: 22
Number of words in Abstract: 213
Number of words in Introduction: 377
Number of words in Discussion: 1058

Abbreviations used are:
CID, collision-induced dissociation; DPP-IV, dipeptidyl peptidase-IV; HPLC, high performance liquid chromatography; LC-MS, liquid chromatography-tandem mass spectrometry; MRM, multiple reaction monitoring; NMR, nuclear magnetic resonance; PCN, pregnenolone-16alpha-carbonitrile.

Abstract

The current study evaluated the potential for two dipeptidyl peptidase-IV (DPP-IV) inhibitor analogues (MRL-A and MRL-B), containing a fluoropyrrolidine moiety in the structure, to undergo metabolic activation. The irreversible binding of these tritium-labeled compounds to rat liver microsomal protein was time- and NADPH-dependent, and was attenuated by the addition of reduced glutathione (GSH) or *N*-acetylcysteine (NAC) to the incubation, indicating that chemically reactive intermediates were formed and trapped by these nucleophiles. Mass spectrometric analyses and further trapping experiments with semicarbazide indicated that the fluoropyrrolidine ring had undergone sequential oxidation and defluorination events resulting in the formation of GSH or NAC conjugates of the pyrrolidine moiety. The bioactivation of MRL-A was catalyzed primarily by rat recombinant cytochrome (CYP) 3A1 and 3A2. Pretreatment of rats with prototypic CYP3A1 and 3A2 inducers (pregnenolone-16alpha-carbonitrile (PCN) and dexamethasone) enhanced the extent of bioactivation, which in turn, led to a higher degree of *in vitro* irreversible binding to microsomal proteins (5- and 9-fold increase, respectively). Herein, we describe studies which demonstrate that the fluoropyrrolidine ring is prone to metabolic activation, and that GSH or NAC can trap the reactive intermediates to form adducts that provide insight into the mechanisms of bioactivation.

Introduction

In recent years, the prevalence of diabetes has increased alarmingly worldwide, giving it the dimension of an epidemic. It is estimated that 140 million people worldwide have diabetes and this figure will increase to 300 million by the year 2025 (King et al., 1998). Type 2 diabetes accounts for ~ 90% of all cases. Current therapeutic strategies for type 2 diabetes include five classes of oral agents – sulfonylureas, biguanides, meglitinides, thiazolidinediones and alpha-glucosidase inhibitors (Loh and Leow, 2002), all of which have their limitations in terms of efficacy and side effects (Riddle, 2003; Tadayyon and Smith, 2003). Over the past few years, multiple approaches have been adopted to develop new therapies for the treatment of Type 2 diabetes. Recent animal and human studies have demonstrated the promise of dipeptidyl peptidase-IV (DPP-IV) inhibitors for improving glucose tolerance (Hinke et al., 2002; Reimer et al., 2002; Sudre et al., 2002; Ahren et al., 2002; Hoffmann et al., 2001). DPP-IV is a membrane-bound and circulating serine protease that can rapidly cleave and inactivate two incretins, namely glucagon-like peptide-1 and gastric inhibitory peptide/glucose-dependent insulinotropic polypeptide (Mentlein, 1999). These gastrointestinal peptides could potentiate glucose-induced insulin secretion by sensitizing pancreatic β-cells to stimulation by glucose. Inactivation of these peptides can be prevented by DPP-IV inhibitors, leading to potentiation of the biological activity of the incretins (Drucker, 2003).

(S)-3-Fluoro-pyrrolidine derivatives are known to be potent and selective inhibitors of DPP-IV (Augustyns et al., 1997). Optimization of derivatives resulting from a series of fluorinated pyrrolidines with 4-substituted cyclohexylglycine subunits resulted

in the selection of MRL-A and MRL-B (Figure 1) as two potent and selective DPP-IV inhibitors with good pharmacokinetic properties and significant activity in an oral glucose tolerance test in lean mice (Caldwell et al., 2004) - favorable characteristics for development consideration at Merck Research Laboratories (MRL). Based on the strategy established at MRL to minimize reactive metabolite formation by structural modification (Evans et al., 2004), evaluation of the metabolic activation potential of these two compounds became of relevance to determine if further lead optimization was needed. Our studies herein described, designed to evaluate the potential for these two compounds to undergo metabolic activation and to understand the mechanism of metabolic activation, indicated that the fluoropyrrolidine ring is the labile site for metabolic activation.

Materials and Methods

Chemicals and Reagents

(1*S*)-1-(*trans*-4-{[(4-trifluoromethoxyphenyl)sulfonyl]amino}cyclohexyl)-2-[(3*S*)-3-fluoropyrrolidin-1-yl]-2-oxoethanaminium chloride (MRL-A), (1*S*)-1-(*trans*-4-{[(2,4-difluorophenyl)sulfonyl]amino}cyclohexyl)-2-[(3*S*)-3-fluoropyrrolidin-1-yl]-2-oxoethanaminium chloride (MRL-B), and a closely related structural analogue used as an internal standard were obtained from the Medicinal Chemistry Department, Merck Research Laboratories, Rahway, NJ. [Benzenesulfonamide-2-^{3}H] MRL-A ([^{3}H]-MRL-A) and [2,4-difluorophenyl-5-^{3}H] MRL-B ([^{3}H]-MRL-B) were synthesized by the Labeled Compound Synthesis Group, Merck Research Laboratory, Rahway, NJ. The radioactive purity (99.4%) was determined by high performance liquid chromatography (HPLC) with a radioactivity detector. *N*-acetylcysteine (NAC), reduced glutathione (GSH), semicarbazide, and NADPH were purchased from Sigma Chemical Co. (St. Louis, MO). A Bicinconinic Acid (BCA) protein assay kit was purchased from Pierce Chemical Co. (Rockford, IL). ScintiSafe Gel and all solvents (HPLC grade) were purchased from Fischer Scientific (Pittsburgh, PA). Liver microsomes prepared from male Sprague-Dawley rats (~250-350 g, ~8 weeks old, n≥10 per group) treated with saline, corn oil, phenobarbital (i.p. injections of 80 mg/kg in saline for 4 days), clofibric acid (i.p. injections of 200 mg/kg in corn oil for 4 days), isoniazid (i.p. injections of 200 mg/kg in saline for 4 days) , pregnenolone-16alpha-carbonitrile (PCN) (i.p. injections of 50 mg/kg in corn oil for 4 days), dexamethasone (i.p. injections of 50 mg/kg in corn oil for 4 days), or 3-methylcholanthrene (3-MC) (i.p. injections of 27 mg/kg in corn oil for 4 days) were purchased from XenoTech LLC (Lenexa, KS).

Irreversible Binding to Rat Liver Microsomal Protein

A pool of 50 male Sprague-Dawley rat (~225-250g, ~8 weeks old) liver microsomes was prepared following procedures described in the literature (Raucy and Lasker, 1991). [^{3}H]-MRL-A (10 μM, 0.14 μCi/nmol) or [^{3}H]-MRL-B (10 μM, 0.14 μCi/nmol) were incubated with rat liver microsomes at 37ºC for 30 and 60 min. The microsomal incubation mixture, in a final volume of 0.2 ml, contained 0.1 M phosphate buffer (pH 7.4), 2 mM $MgCl_2$, 1 mM NADPH, and 1 mg/ml rat liver microsomal protein in the presence and absence of 5 mM GSH or NAC. The reaction was initiated by adding NADPH to the mixture. Control incubations without NADPH were conducted under the same conditions. Determinations of irreversible binding levels were conducted following procedures previously described (Evans et al., 2004). Briefly, incubations were terminated with 800 μl acetone. The precipitated protein was transferred onto a Whatman GF/B filter mat and washed with 80% methanol (1 liter per 48 wells; 20 ml per filter) to remove any radioactive material not covalently bound by using a Brandel cell/membrane harvester (Brandel, Gaithersburg, MA). Protein on the filter paper was then dissolved in 10% sodium dodecyl sulfate overnight at 55ºC. An aliquot was analyzed for protein concentration with the BCA protein assay kit; another aliquot was mixed with ScintiSafe Gel and counted for radioactivity in a Beckman Liquid Scintillation Counter (Model LS6500, Beckman Coulter, Fullerton, CA). The irreversible binding to proteins was expressed as pmol equiv/mg protein from duplicate or triplicate incubations, using the specific activity of the substrate in the incubation mixture and the amount of protein determined for each sample.

In Vitro Incubation Conditions

Rat recombinant CYPs3A1, 3A2, 2B1, 2D1, 1A1, 1A2, 2A2 were purchased from Gentest (Woburn, MA). The incubation mixture contained MRL-A or MRL-B (2, 5, 10, 20, 50 and 100 μM), 0.1 M phosphate buffer (pH 7.4), 2 mM $MgCl_2$, 5 mM GSH or NAC, 1 mg/ml NADPH, and 1 mg/ml microsomal protein or 200 pmol/ml CYP isoform in a total volume of 0.5 ml. Microsomes containing an empty cDNA expression vector were used as control in studies with recombinant CYP isozymes. In the trapping experiments with semicarbazide, semicarbazide (5 mM) was added to the incubations. In the experiments with epoxide hydrolase, microsomal epoxide hydrolase (1 mg protein/ml) was added to the incubations of MRL-A (50 μM) with rat liver microsomes (1 mg/ml) in the presence of 1 mg/ml NADPH and 5 mM NAC. The reaction was initiated by adding NADPH to the mixture and stopped by adding equal volume of ice-cold acetonitrile. Samples were centrifuged at 1850 *g* for 15 min and supernatants were dried under N_2. The residue was reconstituted with mobile phase and analyzed by LC-MS.

Mass Spectrometric Analysis

LC-MS/MS was carried out on either a Perkin-Elmer Sciex API-3000 (Concord, Ontario) triple quadrupole mass spectrometer or a Finnigan LCQ Deca XP mass spectrometer (San Jose, CA), interfaced to a Perkin-Elmer HPLC system (Norwalk, CT) equipped with two Series 200 pumps and a Perkin-Elmer Series 200 autosampler. For metabolite identification, a YMC ODS-AQ column (4.6 x 250 mm, 4.0 μm; Waters Co., Milford, MA) was used. Mobile phases were A, 5 mM ammonium acetate in water with 0.1% formic acid and B, 70% acetonitrile/30% methanol (v/v) with 0.1% formic acid. The flow

rate was 1 ml/min. A linear gradient from 10% B to 70% B in 40 min was applied. The column was washed with 95% B for 5 min, before equilibrating for 8 min with starting conditions. The LC effluent was split with 1/25 directed into the mass spectrometer. LC-MS/MS experiments were conducted using a Turbo-ionspray interface (API-3000) or an electrospray ionization probe (Deca XP) in the positive ion mode. For determining the relative amount of NAC adduct of MRL-A from different incubations, a DASH 8 column (2.1 x 50 mm, 5 μm, Thermo Hypersil-Keystone, Cheshire, UK) was used. Mobile phases were A, 5% acetonitrile/95% water (v/v) in 0.1% acetic acid and B, 5% water/95% acetonitrile (v/v) in 0.1% acetic acid. The flow rate was 1.5 ml/min. A steep linear gradient from 5% B to 90% B in 1.9 min was applied. The multiple reaction monitoring (MRM) transitions monitored were m/z 627 → m/z 164 for the NAC adduct and m/z 468 → m/z 351 for the parent compound MRL-A. The retention time for the NAC adduct was 1.1 min and the retention time for the parent compound was 1.2 min. The peak area ratio of the NAC adduct over internal standard was calculated to indicate the extent of NAC adduct formation.

Accurate mass measurements were performed on a Micromass tandem quadrupole time-of-flight mass spectrometer (Q-TOF) (Beverly, MA). The instrument was operated in the positive ion mode. Mass measurements were based on a lock mass of m/z 609.2812 (the MH^+ ion of reserpine). Samples were introduced by a Hewlett Packard Series 1100 HPLC (Palo Alto, CA) via a Zorbax SB-phenyl column (4.6x150 mm, 5 μm; Agilent Technologies, Wilmington, DE). The mobile phase consisted of A, 5 mM ammonium acetate in water and B, 70% acetonitrile/30% methanol (v/v). The flow rate was

1 ml/min. A linear gradient from 10% B to 95% B in 40 min was applied. The column was washed with 95% B for 5 min, before equilibrating for 8 min with initial conditions.

Results

Irreversible binding of [^{3}H]-MRL-A and [^{3}H]-MRL-B related radioactivity to rat liver microsomes

Incubation of [^{3}H]-MRL-A or [^{3}H]-MRL-B with rat liver microsomes in the presence of NADPH resulted in irreversible binding of radioactivity to microsomal protein. Levels of irreversible binding were 137 and 215 pmol equiv/mg protein for [^{3}H]-MRL-A and 71 and 135 pmol equiv/mg protein for [^{3}H]-MRL-B, after 30 min and 60 min incubations, respectively (Fig. 2). These levels were higher than what is considered an acceptable threshold at MRL (Evans et al., 2004). This time- and NADPH- dependent binding of radioactivity to microsomal protein indicated that both compounds underwent metabolic activation to reactive intermediates that bind to protein irreversibly. Addition of GSH (5 mM) to the incubation did not affect the turnover of MRL-A and MRL-B by rat liver microsomes (data not shown), but significantly lowered the *in vitro* irreversible binding of MRL-A and MRL-B to 62 and 27 pmol equiv/mg protein, respectively, after 60 min incubations (Fig. 2), suggesting that the reactive intermediate(s) formed in the presence of NADPH had been trapped by GSH. *N*-acetylcysteine (NAC), a thiol-based nucleophile that can scavenge electrophilic intermediates, was used in our later studies to trap the reactive intermediate.

Characterization of GSH and NAC adducts formed in rat liver microsomes by LC-MS/MS

The GSH and NAC adducts detected in rat liver microsomal incubations were characterized by comparing their product ion spectra to that of the corresponding parent. The product ion spectra of the parent MRL-A and MRL-B are shown in Fig. 1, where

fragments at *m/z* 351 and 242 from MRL-A are associated with the trifluoromethoxyphenyl sulfonamide moiety, fragments at *m/z* 303 and 194 from MRL-B are associated with the difluorophenyl sulfonamide moiety; the fragment at *m/z* 90 is assigned as the protonated fluoropyrrolidine.

The presence of a MH^+ ion at *m/z* 771 (addition of 303 Da to parent) was observed following full scan analysis of rat liver microsomal incubations of MRL-A in the presence of GSH. Subsequent CID of *m/z* 771 (Fig. 3A) produced product ions at *m/z* 696 and 642, resulting from typical neutral losses of glycine (75 Da) and pyroglutamate (129 Da), respectively (Baillie and Davis, 1993). The fragment ion at *m/z* 753, derived from loss of water, underwent further losses of glycine and pyroglutamate to give rise to the ions at *m/z* 678 and 624, respectively. Fragment ions at *m/z* 308 and 179, corresponding to protonated GSH and subsequent neutral loss of pyroglutamate, respectively, also were observed. The fragment ion at *m/z* 351 in the spectrum indicated that the trifluoromethoxyphenyl sulfonamide cyclohexyl moiety remained intact, suggesting that GSH conjugation had occurred at the fluoropyrrolidine ring. The fragment at *m/z* 446 originated from combined losses of GSH and water.

The corresponding NAC adduct of MRL-A exhibited a protonated molecular ion at *m/z* 627 (addition of 159 Da to parent). The product ion spectrum of the MH^+ at *m/z* 627 (Fig. 3B) showed fragment ions at *m/z* 164 and 122, corresponding to protonated NAC and subsequent neutral loss of ketene (42 Da), respectively. The presence of the fragment at *m/z* 351 further established that NAC was added to the fluoropyrrolidine ring. The fragment ion at *m/z* 231 was assigned as the product arising from cleavage of the amide bond from the parent moiety, resulting in a protonated NAC conjugate of the

fluoropyrrolidine moiety followed by loss of water. The signal at *m/z* 68 could be derived from the ion at m/z 231, with a cleavage at the thioether bond (Fig. 3B).

The GSH adduct of MRL-B had a MH^+ ion at *m/z* 723 (addition of 303 Da to parent). The product ion spectrum of the GSH adduct (Fig. 4A) gave rise to characteristic neutral losses of glycine and pyroglutamate, in addition to loss of water. The fragment ion at *m/z* 303 was consistent with an intact difluorophenyl sulfonamide cyclohexyl moiety in the conjugate, while the signal at *m/z* 398 was assigned as loss of GSH coupled with loss of water. The MH^+ ion of the NAC adduct of MRL-B was at *m/z* 579 (addition of 159 Da to parent). Its product ion spectrum included signals at *m/z* 164, 122, 303, 398, 68 and 231 (Fig. 4B). As discussed above, product ions at *m/z* 303, 68 and 231 indicated that the site of conjugation was the fluoropyrrolidine ring.

Accurate mass determination

Based on the masses of the GSH and NAC adducts, GSH or NAC had added to the fluoropyrrolidine ring of MRL-A or MRL-B with a loss of 2 Da. This was rationalized to occur via two routes: route 1 was postulated to involve dehydrogenation of the fluoropyrrolidine ring (fluorine still present), while route 2 was considered to involve defluorination, with addition of a hydroxyl group. In order to distinguish between these two routes, the accurate mass of the MRL-A-NAC adduct was measured to confirm its elemental composition. The MH^+ ion was observed at *m/z* 627.1746, which was in good agreement with the calculated value of *m/z* 627.1770 when assuming fluorine had been eliminated (-3.8 ppm error). Conversely, dehydrogenation would have resulted in a product of *m/z* 627.1570, leading to a larger error (28 ppm).

Trapping experiments with semicarbazide

Following incubations of MRL-A with rat liver microsomes in the presence of NADPH, an oxidative metabolite (M1) was detected. The product ion scan of *m/z* 484 (addition of 16 Da to parent) gave rise to a fragment ion at *m/z* 466 derived from loss of water, and a fragment ion at *m/z* 351 consistent with an intact trifluoromethoxyphenyl sulfonamide cyclohexyl moiety in the metabolite (Fig. 5A), collectively suggesting that hydroxylation occurred on the fluoropyrrolidine moiety. Addition of semicarbazide (5 mM), a trapping agent for aldehydes, to the incubation resulted in the formation of a semicarbazide adduct (MH^+ at *m/z* 541), with significant reduction in the formation of M1 (Fig. 6), suggesting that M1 was converted to the semicarbazide adduct. This adduct was not detected in the incubations in the absence of semicarbazide. The MS/MS spectrum of the MH^+ ion at *m/z* 541 consisted of fragment ions at *m/z* 521, 466, and 446, derived from neutral losses of 20 Da (-HF) and 75 Da (-semicarbazide), and combined losses (-HF-semicarbazide), respectively, and the fragment ion at m/z 351 (Fig. 5B). It is very likely that the product (M1) was hydroxylated at C-5 or C-2, which would allow it to be in equilibrium with a ring-opened aldehyde that can be trapped by semicarbazide (Scheme 1A).

Incubations of MRL-A with rat liver microsomes (in the presence of NADPH) enriched with both NAC and semicarbazide generated a semicarbazide adduct of NAC conjugate (MH^+ at *m/z* 684). CID of the MH^+ at *m/z* 684 resulted in fragment ions at *m/z* 231, 446, and 609 (Fig. 5C), suggesting the presence of aldehyde group trapped by semicarbazide in the NAC conjugate.

Identification of CYP enzymes involved in the formation of the NAC adduct of MRL-A

The extent of formation of NAC adduct of MRL-A was semi-quantified as peak area ratio of NAC adduct of MRL-A over internal standard. No attempts were made in the present studies to quantify accurately the NAC adduct formed, since the turnover of substrate to the detectable product was low. When MRL-A was incubated with rat recombinant CYPs1A1, 1A2, 2B1, 2D1, 2A2, 3A1, 3A2 in the presence of NADPH and NAC, the NAC adduct was formed most abundantly from incubations that contained CYP3A1 or CYP3A2 (Table 1), indicating that rat CYP3A1 and CYP3A2 are the major isoforms catalyzing the metabolic activation of MRL-A. The extent of formation of the NAC adduct by CYP3A1 was dependent on substrate concentration investigated (2-100 μM), with a maximal rate being observed at 50 μM (data not shown).

Irreversible binding of [^{3}H]-MRL-A related radioactivity to liver microsomes from rats pre-treated with different CYP inducers

The irreversible binding of [^{3}H]-MRL-A related radioactivity to rat liver microsomes in the presence of NADPH was increased about 5- or 9-fold when the liver microsomes used had been prepared from rats treated with PCN or dexamethasone, respectively (Fig. 7). A 3-fold increase in the irreversible binding was observed in liver microsomes prepared from rats pretreated with phenobarbital (Fig. 7). Pre-treatment of rats with 3-methylcholanthrene (3-MC) or clofibric acid had little or no effect on the level of the *in vitro* irreversible binding determined for MRL-A (Fig. 7), while treatment of rats with isoniazid seemed to decrease these levels (Fig. 7). The irreversible binding to the

above rat liver microsomes was significantly reduced by the presence of NAC (5 mM) in the incubation mixture (Fig. 7).

Formation of the NAC adduct of MRL-A in rat liver microsomes from rats pre-treated with different inducers

The NAC adduct of MRL-A was formed most abundantly in liver microsomes from PCN- or dexamethasone-treated rats, followed by liver microsomes from phenobarbital-treated rat (Table 2). The yield of the NAC adduct was the lowest in liver microsomes from rats treated with isoniazid, where the lowest *in vitro* irreversible binding (50 pmol/mg protein) was also observed (Table 2).

There was a good correlation between the formation of an aldehyde group trapped by semicarbazide as a semicarbazide adduct and the formation of NAC conjugate of MRL-A in the liver microsomes prepared from rats treated with different inducers (Fig. 8).

Discussion

The current studies evaluated the metabolic activation potential of two compounds from a series of fluorinated pyrrolidines with 4-substituted cyclohexylglycine subunits, MRL-A and MRL-B, which had been optimized for DPP-IV inhibition and selectivity with good pharmacokinetic properties in rats and significant efficacy in an oral glucose tolerance test in lean mice. Our studies demonstrated that incubations of MRL-A and MRL-B with rat liver microsomes resulted in irreversible binding levels in excess of the 50 pmol eq/mg protein typically considered acceptable at MRL (Evans et al., 2004). In addition, substrate turnover in rat liver microsomes was low, suggesting that most of the turnover of the compound was being metabolically activated.

The similar fragmentation patterns observed from the GSH/NAC adducts of MRL-A and MRL-B (Figs 3, 4) suggested the same bioactivation mechanism was involved, with the fluoropyrrolidine ring as the labile site. It has been shown that compounds containing a pyrrolidine ring can be bioactivated via formation of an iminium ion intermediate, which, in most cases, can be trapped by cyanide (Streeper et al., 1997). In our studies, cyanide had little or no effect on the irreversible binding (data not shown), suggesting that this metabolic activation pathway may not play an important role in the irreversible binding to protein.

The accurate mass determined for the NAC adduct of MRL-A indicated that defluorination and oxidation events were involved in the metabolic activation of the fluoropyrrolidine ring. Furthermore, the presence of an aldehyde group in the NAC conjugate, and the positive correlation observed between the formation of an aldehyde group (trapped by semicarbazide) and the formation of NAC conjugate (Fig. 8), indicated

that aldehyde formation played a role in the bioactivation. One of the proposed mechanisms involved hydroxylation at C-5, leading to a ring-opened β-fluoroaldehyde, which in turn may undergo elimination of HF to form an α, β-unsaturated aldehyde as the electrophilic intermediate. Nucleophiles such as GSH or NAC would then attack the intermediate via a Michael addition mechanism to form the GSH or NAC conjugate, in which the aldehyde group could be trapped by semicarbazide. The aldehyde group may also cyclize with the amide nitrogen to form the ring-closed hydroxylated derivative in a reversible manner (Scheme 1A).

An alternative mechanism for the bioactivation of the fluoropyrrolidine that was taken into consideration (Scheme 1B) involved initial hydroxylation beta to the carbon (C-4) attached to fluorine, followed by elimination of the fluoride anion upon intramolecular attack by the β-hydroxyl group resulting in the formation of an epoxide. GSH or NAC then would attack the epoxide yielding the GSH or NAC adducts. However, when microsomal incubations enriched with NAC were conducted in the presence or absence of microsomal epoxide hydrolase (1 mg protein/ml), no significant alteration in the formation of NAC adduct was observed with or without epoxide hydrolase (data not shown). Possible reasons for this observation could be that the epoxide pathway did not play a role in the metabolic activation process, or that the epoxide intermediate proposed here was not a substrate of or not accessible to the epoxide hydrolase used in this study. However, the current data indicated the formation of a semicarbazide conjugate, which cannot be accommodated by the pathway illustrated in Scheme 1B, further supporting the conclusion that the bioactivation of MRL-A and MRL-B occurred via pathway A.

NMR analysis was attempted on the isolated NAC adduct of MRL-A. The ^{1}H-NMR spectrum was however too complex to interpret because of the presence of potential multiple species arising from multiple stereoconfigurations, existing as two rotamers around the pyrrolidine N-CO amide bond.

The formation of the reactive electrophilic intermediate trapped by NAC was catalyzed primarily by rat recombinant CYP3A1 and CYP3A2 (Table 1). Dexamethasone and PCN are potent inducers of rat CYP3A1 and CYP3A2 (Parkinson, 2001). Accordingly, the bioactivation potential of MRL-A in liver microsomes from rats pretreated with these inducers was increased significantly, as indicated by the high level of the *in vitro* irreversible binding and the high level of the NAC adduct detected (Table 2). The moderate increase in the irreversible binding of radioactivity to liver microsomes from rats treated with phenobarbital could be attributed to the moderate inductive effect of phenobarbital on CYP3A2 (Parkinson, 2001). CYPs1A1 and 1A2 had little or no role in the metabolic activation of MRL-A (Table 1). Consistent with that, treatment of rats with 3-MC, a potent inducer of CYP1A1 and CYP1A2 (Parkinson, 2001), had little or no effect on the *in vitro* irreversible binding determined for [^{3}H]-MRL-A (Fig. 7). No increase in the *in vitro* irreversible binding was observed with liver microsomes from rats pretreated with clofibric acid (Fig. 7), an inducer of CYP4A (Parkinson, 2001). This lack of effect could be due to the fact that CYP4A enzymes are not responsible for the bioactivation, or that there is competition between the bioactivation pathway and alternative metabolic pathways for MRL-A, as clofibric acid is also an inducer of other enzymes (Fournel et al., 1983). Treatment of rats with isoniazid decreased the *in vitro* irreversible binding to some extent (Fig. 7). It is possible that CYP2E1, which is induced

by isoniazid (Parkinson, 2001), might increase alternative metabolic pathways, thus decreasing the substrate availability for bioactivation.

A good correlation was observed between the formation of the NAC adduct of MRL-A and the *in vitro* irreversible binding of [^{3}H]-MRL-A in liver microsomes from rats pretreated with different inducers (Table 2), suggesting that, in the context of the present study, formation of reactive intermediates identified as GSH or NAC adducts could serve as an index for the potential of irreversible binding.

The chemically reactive intermediates studied herein are responsible for the irreversible binding to microsomal protein *in vitro*, implying that these fluoropyrrolidine derivatives might have the potential to covalently bind to proteins or other macromolecules *in vivo*. It has been shown that covalently modified protein may interrupt normal cellular functions, or function as haptens causing idiosyncratic drug reactions (Uetrecht, 1999). Moreover, the reactive metabolites that can be scavenged by GSH may deplete cellular GSH resulting in alterations in the redox state of the cell and subsequently causing oxidative stress in cells with progression to cell injury (Nelson and Pearson, 1990). Given the potential liability of chemically reactive electrophilic metabolites, it is reasonable to attempt to minimize the potential of bioactivation through structural modification at the early stage of drug discovery (Baillie and Kassahun, 2001; Evans et al., 2004).

Acknowledgments

We thank Ping Chen, Dr. Emma Parmee, Jiafang He and Dr. Ann Weber of the Basic Chemistry Department for providing the compounds, and Drs. Ashok Chaudhary and Dennis Dean of the Radiosynthesis Group for providing tritium-labeled materials. We thank Dr. Zhoupeng Zhang of the Drug Metabolism Department for helpful discussions. We thank Dr. Magang Shou and Yinhe Li of the Drug Metabolism Department for providing rat recombinant CYP 3A1. We thank the reviewers of the DMD journal for their insightful comments to the study.

References

Augustyns KJL, Lambeir AM, Borloo M, De Meester I, Vedernikova I, Vanhoof G, Hendriks D, Scharpé S and Haemers A (1997) Pyrrolidides: synthesis and structure-activity relationship as inhibitors of dipeptidyl peptidase IV. *Eur J Med Chem* 32:301-309.

Ahren B, Simonsson E and Larsson H (2002) Inhibition of dipeptidyl peptidase IV improves metabolic control over a 4-week study period in type 2 diabetes. *Diabetes Care* 25:869-875.

Baillie TA and Davis MR (1993) Mass spectrometry in the analysis of glutathione conjugates. *Biol Mass Spectrom* 22:319-325.

Baillie TA and Kassahun K (2001) Biological reactive intermediates in drug discovery and development: a perspective from the pharmaceutical industry. *Adv Exp Med Biol* 500:45-51.

Caldwell CG, Chen P, He J, Parmee ER, Leiting B, Marsilio F, Patel RA, Wu JK, Eiermann GJ, Petrov A, He H, Lyons KA, Thornberry NA and Weber AE (2004) Fluoropyrrolidine amides as dipeptidyl peptidase IV inhibitors. *Bioorganic Med Chem Letters* 14:1265-1268.

Drucker DJ (2003) Therapeutic potential of dipeptidyl peptidase IV inhibitors for the treatment of type 2 diabetes. *Expert Opin Investig Drugs* 12(1):87-100.

Evans DC, Watt AP, Nicoll-Griffith DA, Baillie TA (2004) Drug-protein adducts: an industry perspective on minimizing the potential for drug bioactivation in drug discovery and development. *Chem Res Toxicol* 17(1):3-16.

Fournel S, Magdalou J, Batt AM, Siest G (1983) Comparative study of four hypolipidaemic agents on the activity of drug-metabolizing enzymes in rat liver microsomes. *Int J Clin Pharmacol Res* 3(6):431-436.

Hinke SA, Gelling RW, Pederson RA, Manhart S, Nian C, Demuth HU and McIntosh CHS (2002) Dipeptidyl peptidase IV – Resistant glucose-dependent insulinotropic polypeptide improves glucose tolerance in normal and obese diabetic rats. *Diabetes* 51:652-661.

Hoffmann T, Glund K and McIntosh CHS (2001) DPPIV inhibition as treatment of type II diabetes, in *Cell-surface aminopeptidases: basic and clinical aspects* (S Mizutani Ed.) pp381-387, Elsevier, New York.

King H, Auber RE and Herman WH (1998) Global burden of diabetes, 1995-2005: prevalence, numerical estimates and projections. *Diabetes Care* 21: 1414-31.

Loh KC and Leow MK (2002) Current therapeutic strategies for type 2 diabetes mellitus. *Ann Acad Med Signapore* 31:722-729.

Mentlein R (1999) Dipeptidyl-peptidase IV (CD26) – role in the inactivation of regulatory peptides. *Regul Pept* 85:9-24.

Nelson SD and Pearson PG (1990) Covalent and noncovalent interactions in acute lethal cell injury caused by chemicals. *Annu Rev Pharmacol Toxicol* 30:169-195.

Parkinson A (2001) Biotransformation of xenobiotics, in *Casarett and Doull's Toxicology: The Basic Scientific of Poisons* (Klaassen CD Ed), pp133-124, McGraw-Hill, New York.

Raucy JL and Lasker JM (1991) Isolation of P450 enzymes from human liver. *Methods Enzymol* 206:557-587.

Reimer MK, Holst JJ and Ahren B (2002) Long-term inhibition of dipeptidyl peptidase IV improves glucose tolerance and preserves islet function in mice. *Eur J Endocrinol* 146:717-727.

Riddle MC (2003) Sulfonylureas differ in effects on ischemic preconditioning – is it time to retire glyburide? *J Clin Endocrinol Metab* 88:528-530.

Streeper RT, Pearson PG, Zhao Z, Mizsak SA, Sanders PE, Wienkers LC and Vrbanac JJ (1997) In vitro metabolic transformations of 2,4-dipyrrolidinylpyrimidine: a chemical probe for P450-mediated oxidation of tirilazad mesylate. *Xenobiotica* 27:1131-1145.

Sudre B, Broqua P, White RB, Ashworth D, Evans DM, Haigh R, Junien JL and Aubert ML (2002) Chronic inhibition of circulating dipeptidase IV by FE999011 delays the occurrence of diabetes in male Zucker diabetic fatty rats. *Diabetes* 51:1461-1469.

Tadayyon M and Smith SA (2003) Insulin sensitisation in the treatment of type 2 diabetes. *Expert Opin Investig Drugs* 12:307-324.

Uetrecht JP (1999) New concepts in immunology relevant to idiosyncratic drug reactions: the “danger hypothesis and innate immune system. *Chem Res Toxicol* 12:387-395.

List of Figures

The two points in the plot corresponding to the higher levels of formation of NAC adduct and of formation of semicarbazide adduct were observed in liver microsomes prepared from dexamethasone and PCN treated rats.

Scheme 1. Possible mechanisms for the metabolic activation of MRL-A and MRL-B. Pathway A was supported by the data.

Table 1. Formation of the NAC adduct of MRL-A by rat recombinant CYP isoforms.

CYP Isoform	Formation of NAC adduct (peak area ratio from MRM data)
1A1	0.01
1A2	0.02
2A2	0.00
2B1	0.00
2D1	0.01
3A1	1.20
3A2	0.24
Control	0.00

The formation of the NAC adduct was calculated as the peak area ratio of the NAC adduct over internal standard obtained from MRM data. Data represent mean from duplicate incubations.

Table 2. Formation of the NAC adduct of MRL-A following *in vitro* incubation with liver microsomes from rats pretreated with different inducers.

Treatment	Formation of NAC adduct (peak area ratio from MRM data)	Irreversible Binding (pmol equiv/mg protein)
Saline	0.05	164
Isoniazid	0.02	50
Clofibric Acid	0.06	154
Phenobarbital	0.14	474
Corn oil	0.04	135
3-MC	0.04	180
PCN	0.23	729
Dexamethasone	0.31	1246

The formation of the NAC adduct was calculated as the peak area ratio of the NAC adduct over internal standard obtained from MRM data. Data represent the mean from duplicate incubations.

Scheme 1

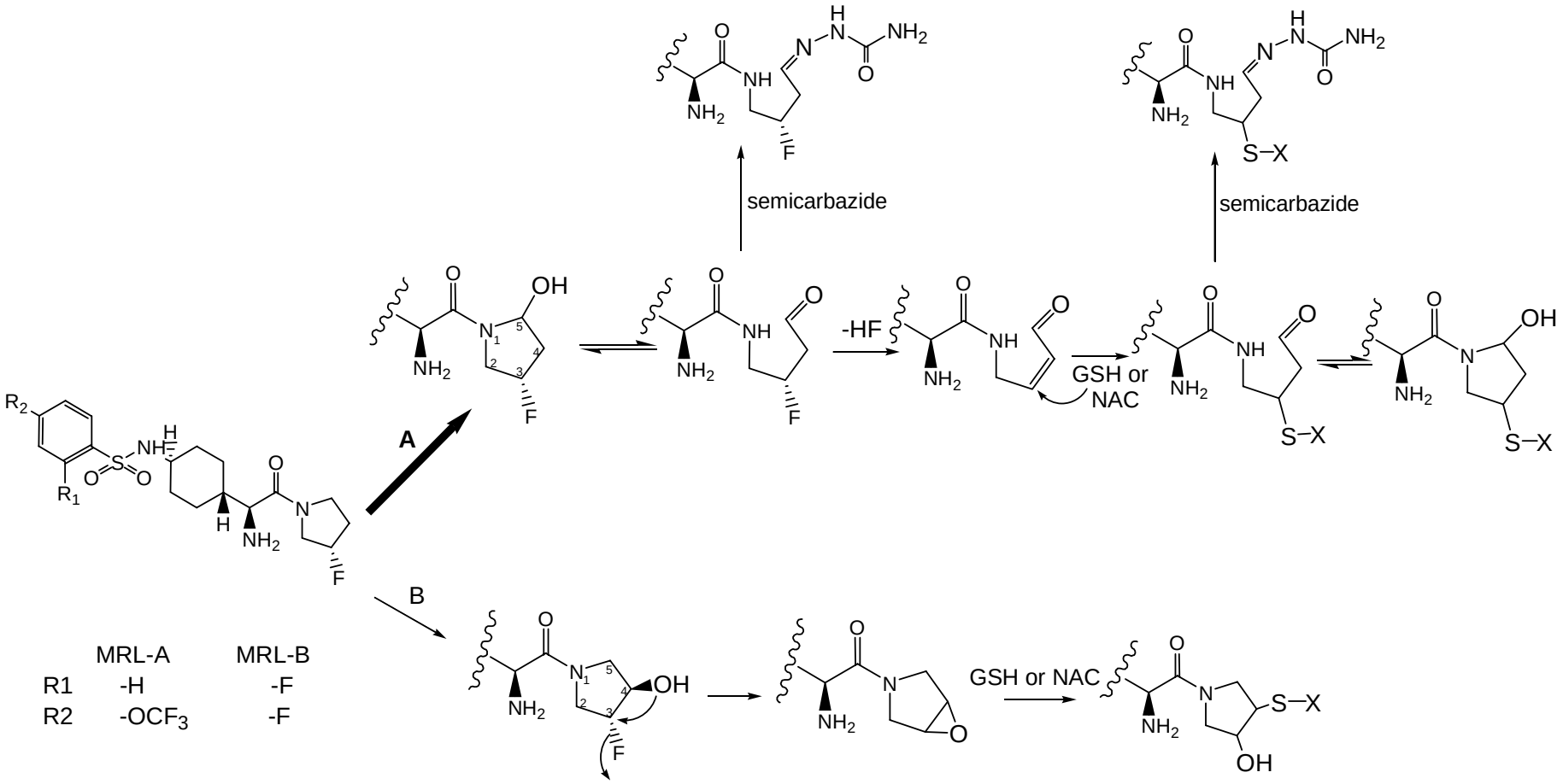
semicarbazide
semicarbazide
-HF
GSH or
NAC
A
B
GSH or NAC
MRL-A MRL-B
R1 -H -F
R2 -OCF3 -F
X: GSH or NAC

Fig. 1

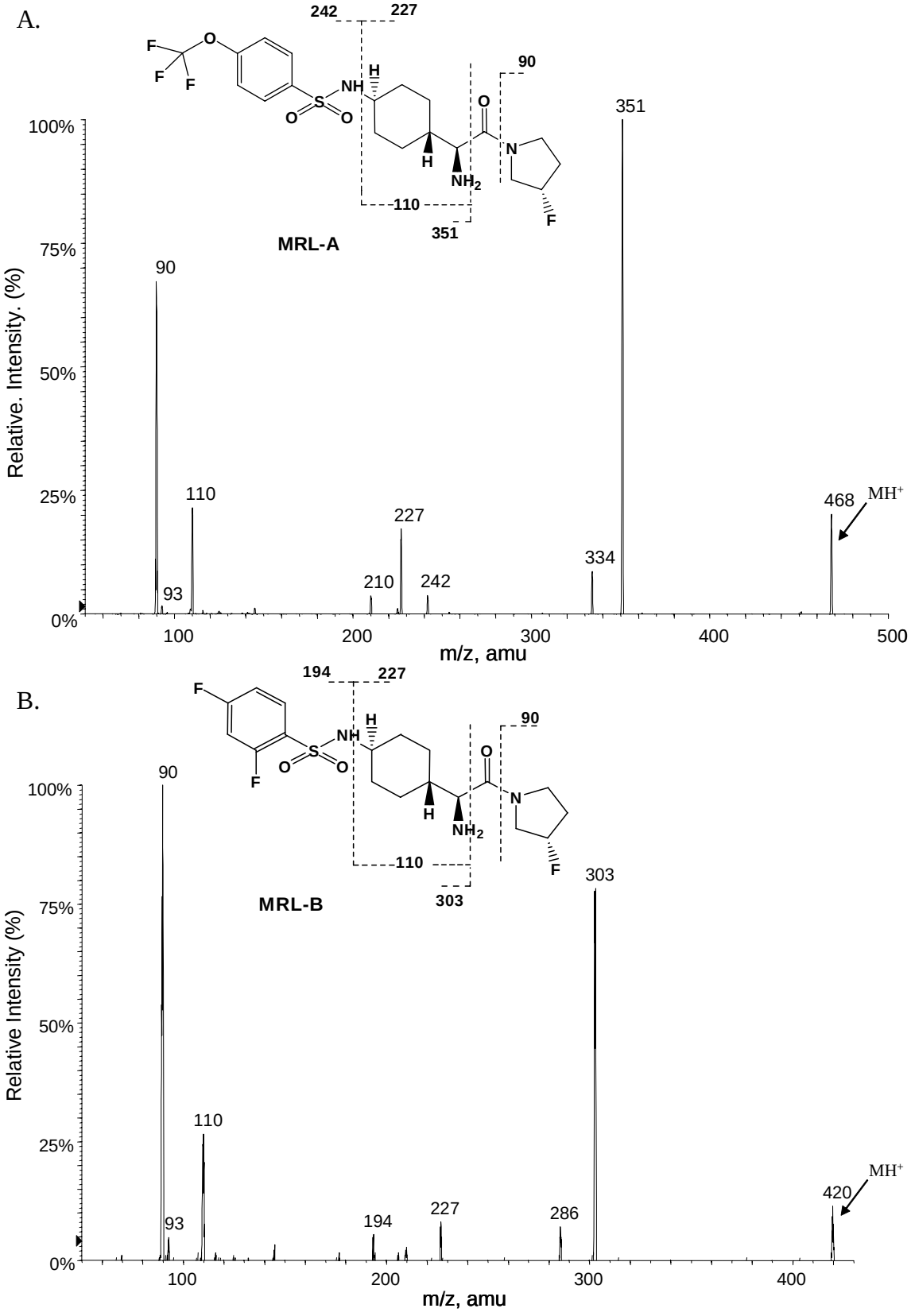
A.
242
227
90
351
110
351
MRL-A
100%
75%
50%
25%
0%
Relative. Intensity. (%)
90
110
227
210
242
93
334
351
468
MH+
100
200
300
400
500
m/z, amu
B.
194
227
90
303
110
303
MRL-B
Relative Intensity (%)
90
110
93
194
227
286
303
420
MH+
m/z, amu

Fig. 2

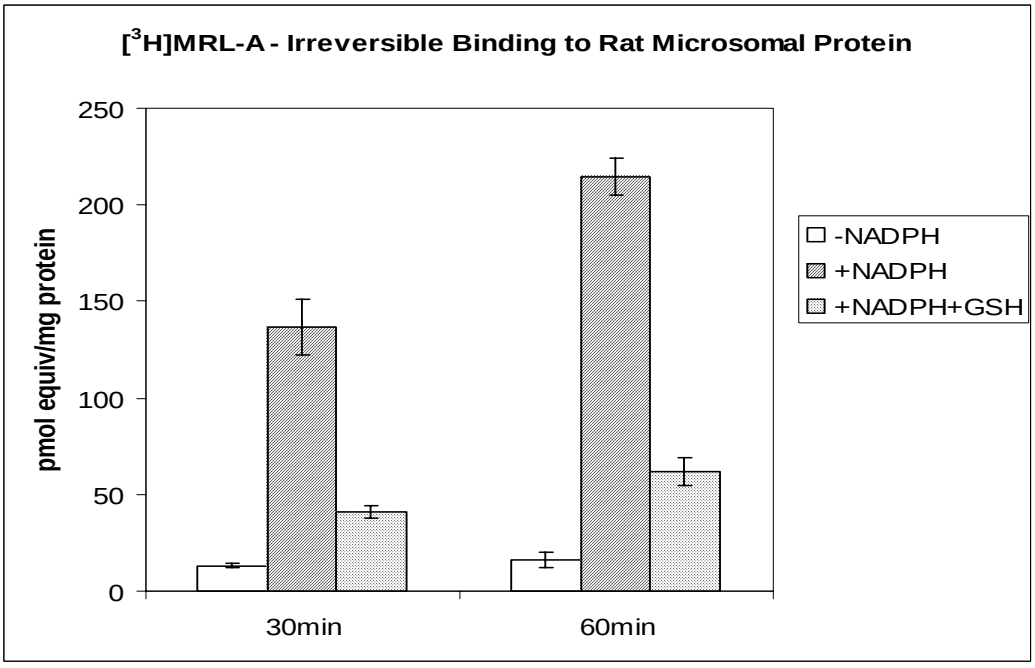
[3H]MRL-A - Irreversible Binding to Rat Microsomal Protein
pmol equiv/mg protein
250
200
150
100
50
0
30min
60min
-NADPH
+NADPH
+NADPH+GSH

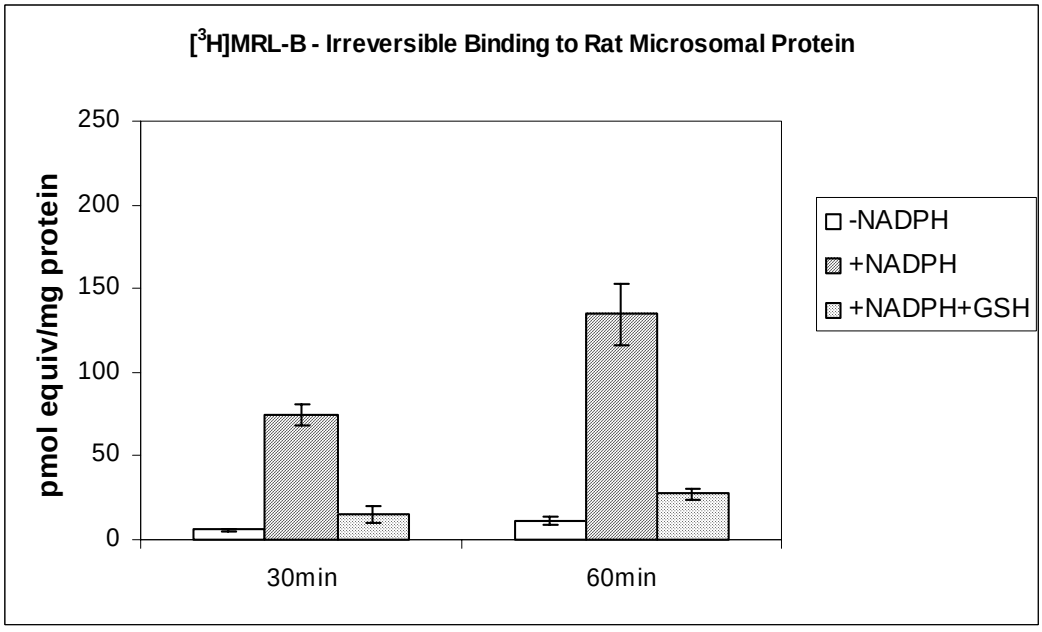
[3H]MRL-B - Irreversible Binding to Rat Microsomal Protein
pmol equiv/mg protein
250
200
150
100
50
0
30min
60min
-NADPH
+NADPH
+NADPH+GSH

Fig. 3

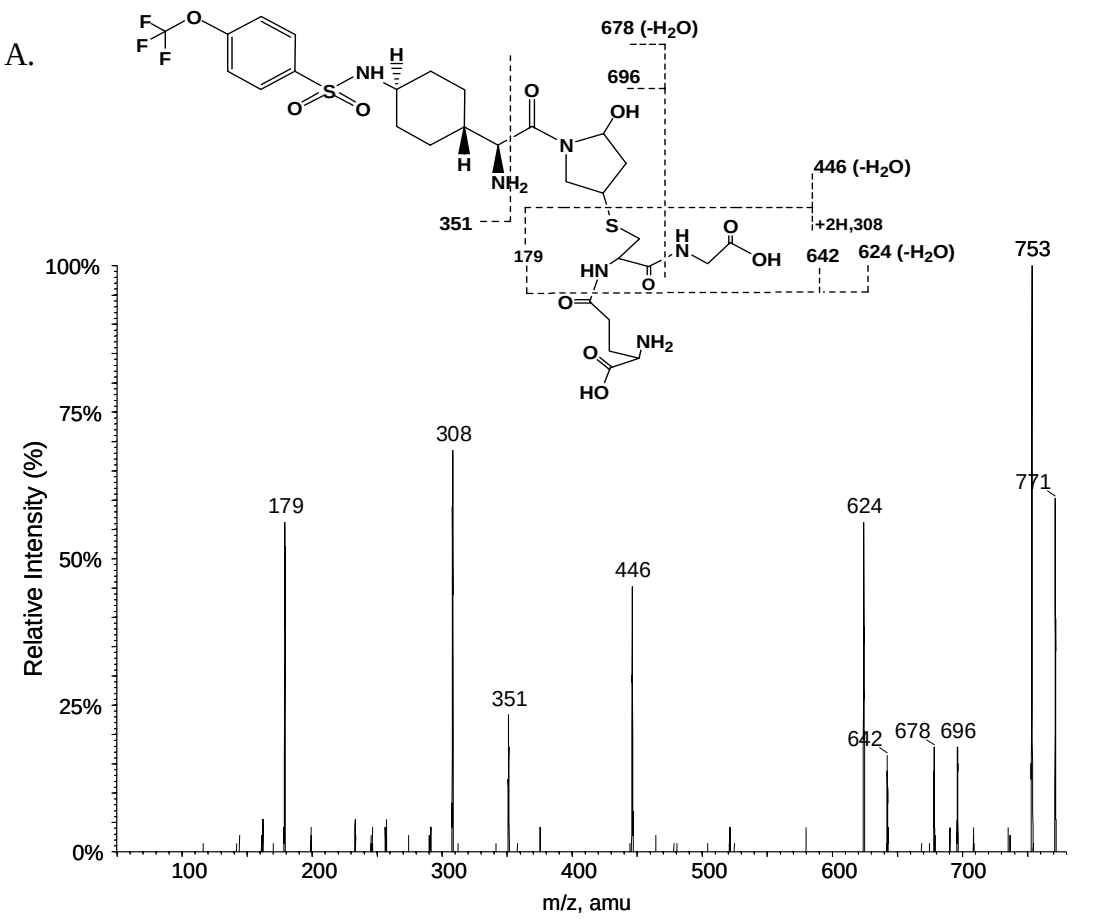
A.
678 (-H2O)
696
446 (-H2O)
351
+2H,308
179
642
624 (-H2O)
753
771
624
308
179
446
351
642
678
696
100%
75%
50%
25%
0%
Relative Intensity (%)
100
200
300
400
500
600
700
m/z, amu

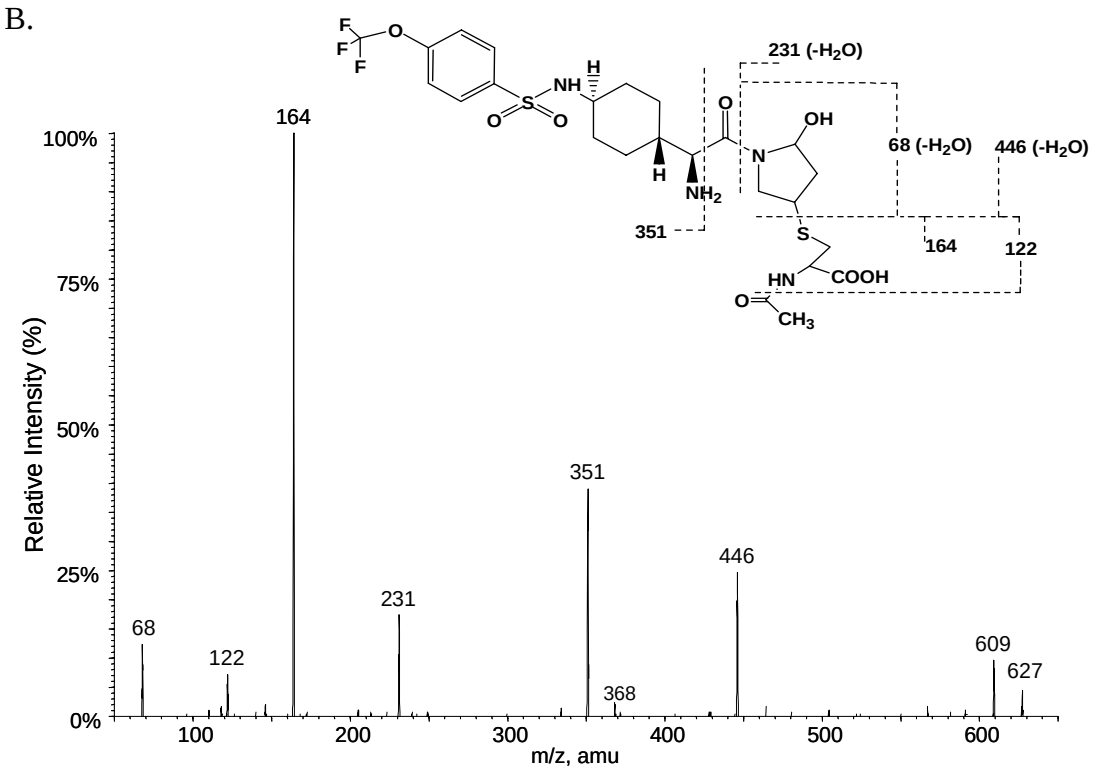
B.
231 (-H2O)
68 (-H2O)
446 (-H2O)
351
164
122
164
351
446
231
68
122
609
627
368
100%
75%
50%
25%
0%
Relative Intensity (%)
100
200
300
400
500
600
m/z, amu

Fig. 4

A.

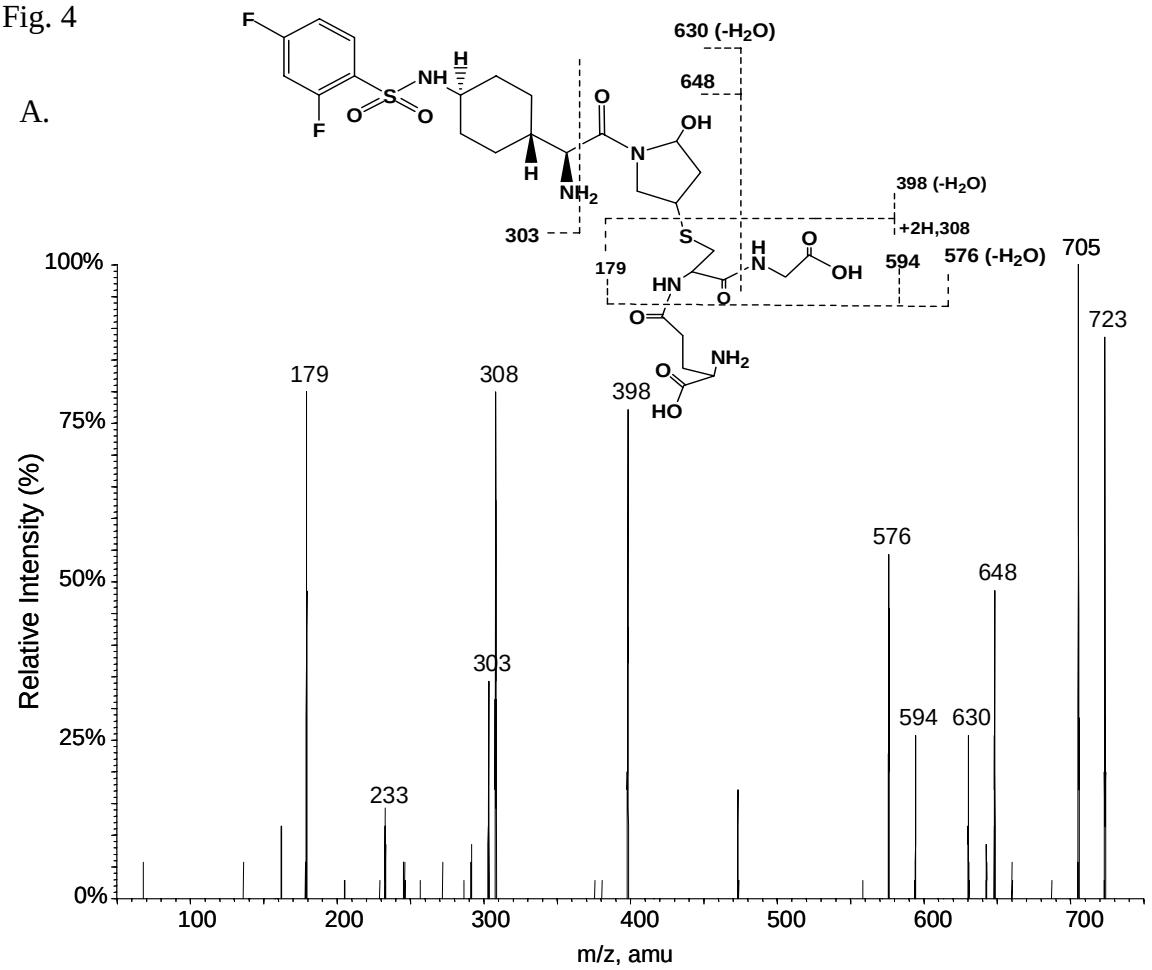
630 (-H2O)
648
398 (-H2O)
+2H,308
303
179
594
576 (-H2O)
705
723
100%
75%
50%
25%
0%
Relative Intensity (%)
179
308
398
576
648
303
594
630
233
100
200
300
400
500
600
700
m/z, amu

B.

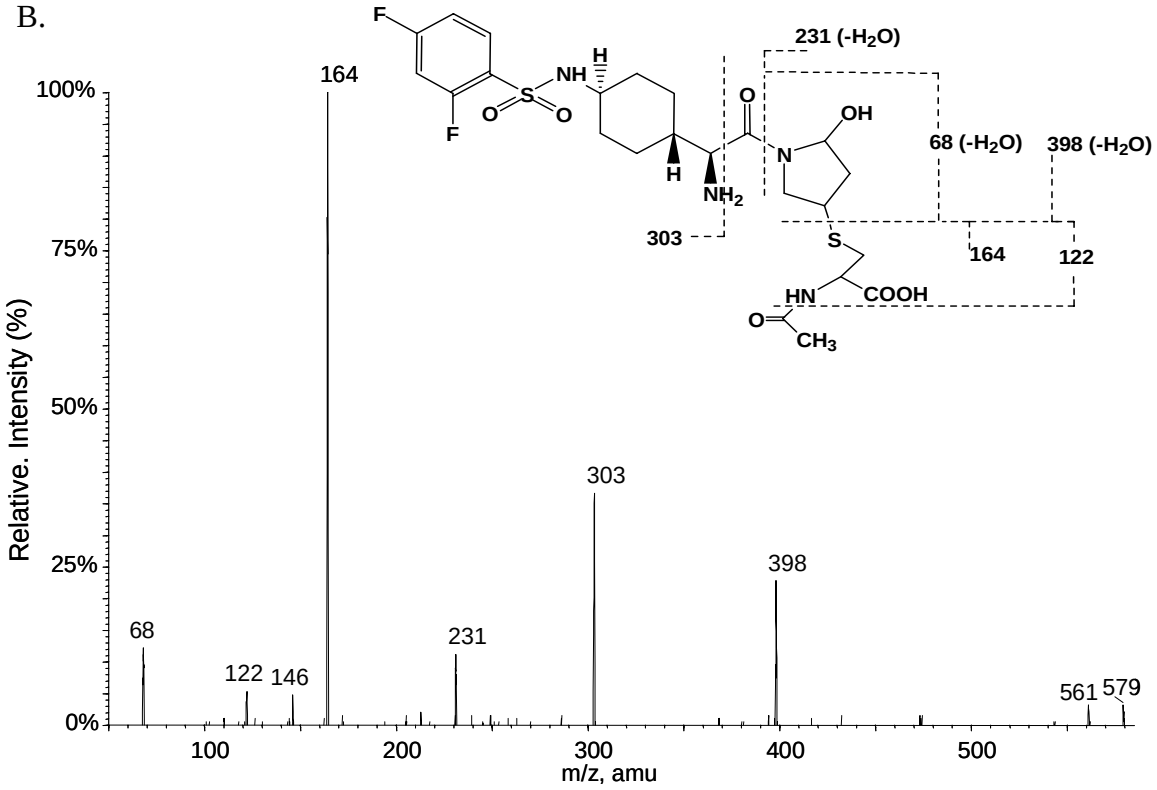
231 (-H2O)
164
68 (-H2O)
398 (-H2O)
303
164
122
100%
75%
50%
25%
0%
Relative. Intensity (%)
303
398
68
231
122
146
561
579
100
200
300
400
500
m/z, amu

Fig. 5

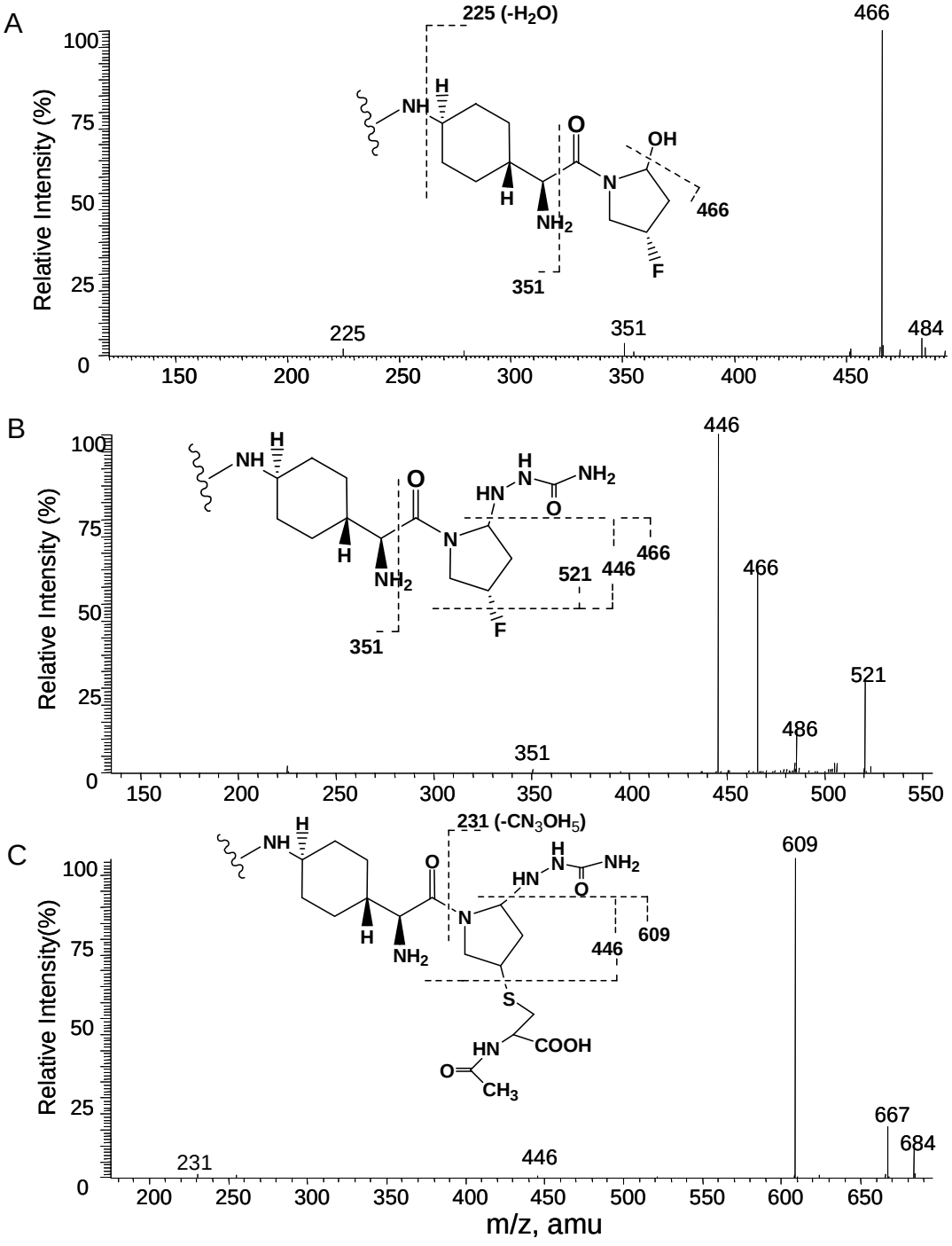
A
225 (-H2O)
466
Relative Intensity (%)
225
351
484
B
446
466
521
486
351
C
231 (-CN3OH5)
609
667
684
231
446
Relative Intensity(%)
m/z, amu

Fig. 6

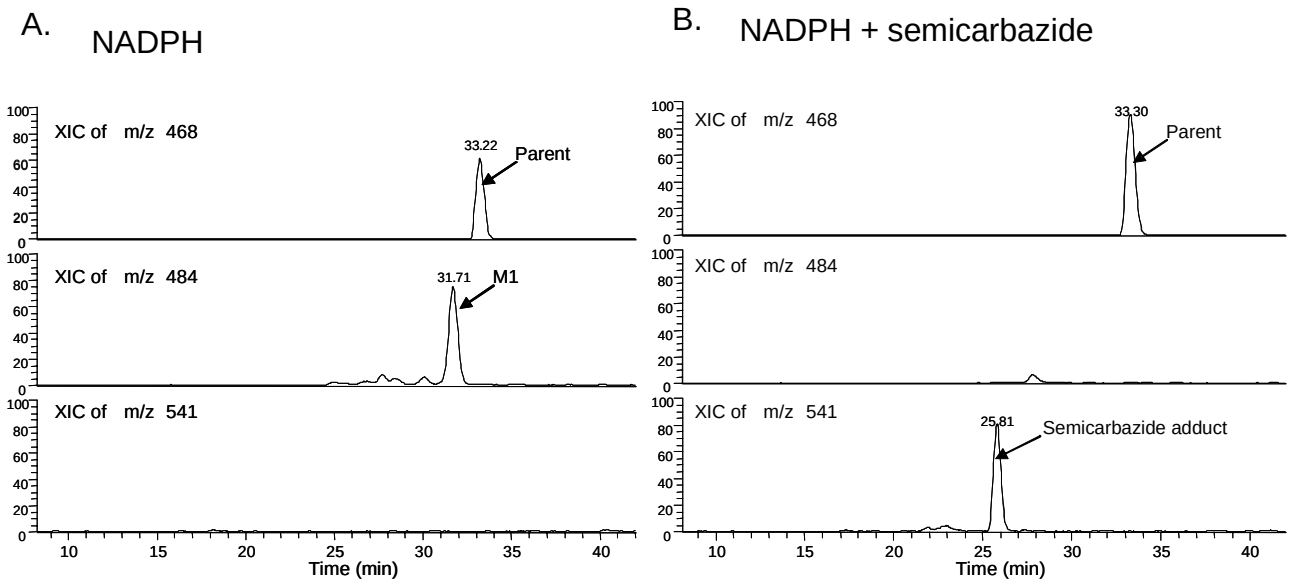
A.
NADPH
XIC of m/z 468
33.22
Parent
XIC of m/z 484
31.71
M1
XIC of m/z 541
Time (min)
B.
NADPH + semicarbazide
XIC of m/z 468
33.30
Parent
XIC of m/z 484
XIC of m/z 541
25.81
Semicarbazide adduct
Time (min)

Fig. 7

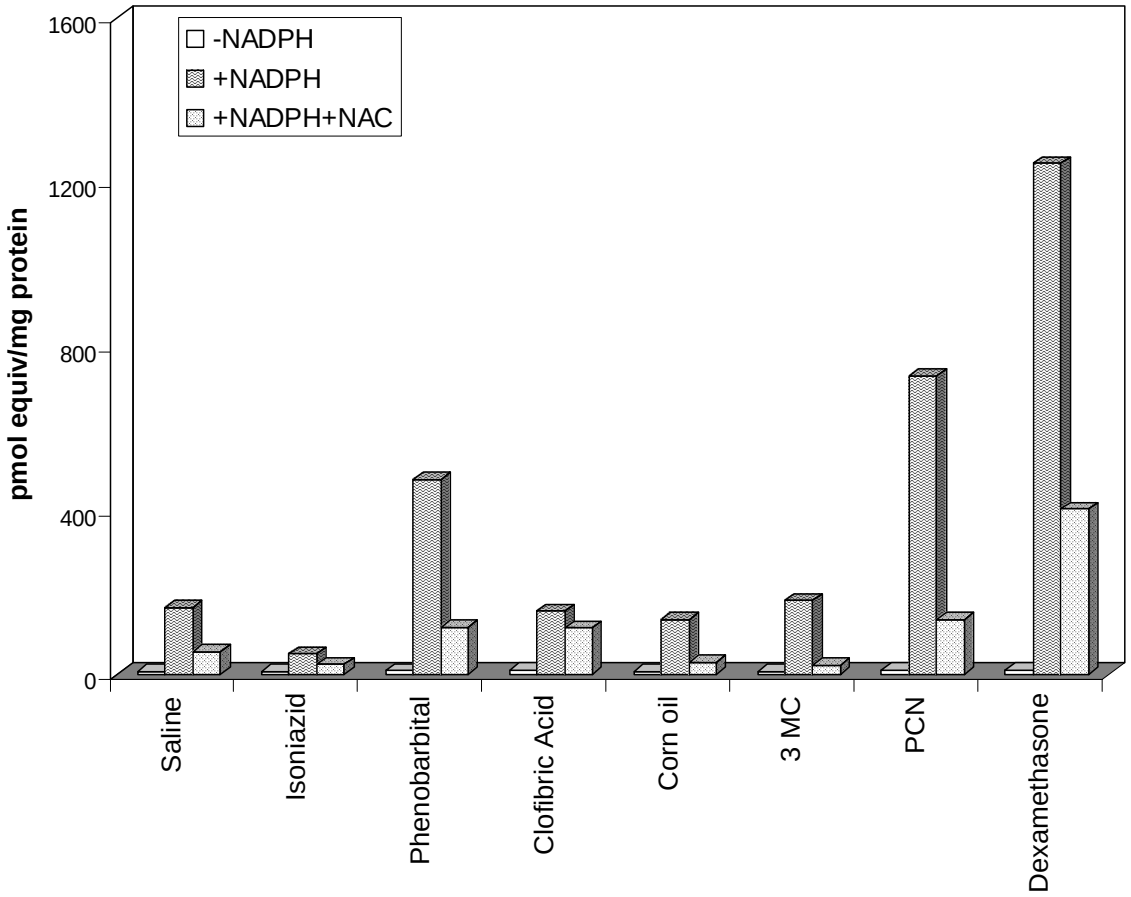
-NADPH
+NADPH
+NADPH+NAC
pmol equiv/mg protein
1600
1200
800
400
0
Saline
Isoniazid
Phenobarbital
Clofibric Acid
Corn oil
3 MC
PCN
Dexamethasone

Fig. 8

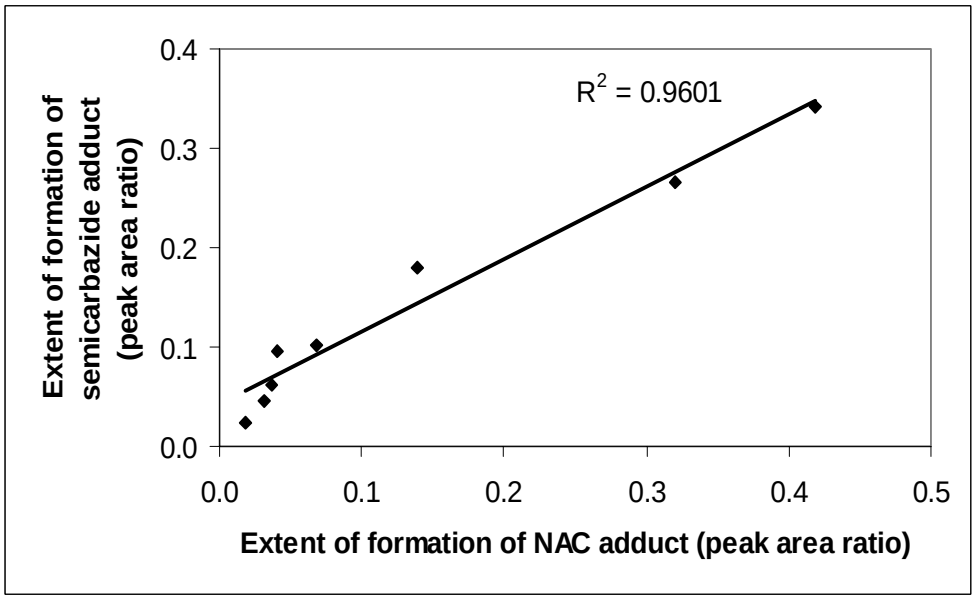
Extent of formation of semicarbazide adduct (peak area ratio)
0.4
0.3
0.2
0.1
0.0
R2 = 0.9601
0.0
0.1
0.2
0.3
0.4
0.5
Extent of formation of NAC adduct (peak area ratio)